

Constraining hybrid inflation models with WMAP three-year results

Antonio Cardoso*

Institute of Cosmology and Gravitation, University of Portsmouth, Portsmouth, PO1 2EG, United Kingdom

(Dated: December 2, 2024)

We reconsider the original model of quadratic hybrid inflation in light of the WMAP three-year results and study the possibility of obtaining a spectral index of primordial density perturbations, n_s , smaller than one from this model. The original hybrid inflation model naturally predicts $n_s \geq 1$ in the false vacuum dominated regime but it is also possible to have $n_s < 1$ when the quadratic term dominates. We therefore investigate whether there is also an intermediate regime compatible with the latest constraints, where the scalar field value during the last 50 e-folds of inflation is less than the Planck scale.

I. INTRODUCTION

The results from the WMAP three-year data [1] have provided the first indication that the spectral index of primordial density perturbations, n_s , is smaller than one. The original hybrid inflation model [2] naturally predicts $n_s \geq 1$ in the false vacuum dominated regime but it is also possible to have $n_s < 1$ when the quadratic term dominates [3]. We are therefore interested in whether there is also an intermediate regime compatible with the latest constraints. Hybrid inflation models are attractive from a theoretical point of view because the inflaton field ϕ is far below the Planck scale during inflation, in the false vacuum dominated regime, which makes these models easier to implement within supergravity [4]. Therefore we also investigate whether there is an intermediate regime where the scalar field value during the last 50 e-folds of inflation is less than the Planck scale.

In this paper we study the original hybrid inflation model with a quadratic potential for the inflaton. We want to analyze carefully this model in light of the new WMAP results, exploring the space of parameters of the model. We have run a code to calculate numerically the spectral tilt of the scalar curvature perturbations, n_s , the running of the spectral tilt, α_s , and the tensor to scalar ratio, r , assuming slow-roll, for a specific region of parameters of the model. We study the cases for which we have $n_s < 1$ and compare the results obtained with the WMAP three-year results. We use the 68% and 95% confidence level contours from WMAP only and WMAP + SDSS taken from [5]. Recently a similar work has used the WMAP three-year results to put constraints on hybrid inflation models [6].

We also study the inverted hybrid inflation model [7] with a quadratic potential for the inflaton (see Appendix).

II. THE HYBRID INFLATION MODEL

The potential for the hybrid inflation model is given by [3]

$$V(\phi, \chi) = \frac{1}{4}\lambda(\chi^2 - \chi_0^2)^2 + \frac{1}{2}m^2\phi^2 + \frac{1}{2}\lambda'\phi^2\chi^2, \quad (1)$$

where ϕ is the inflaton, χ is called the “waterfall” field, λ and λ' are coupling constants and χ_0 and m are constant masses.

It is assumed that χ stays at the origin, which corresponds to a false vacuum, while ϕ rolls down from a initially large (positive) value until it reaches a critical value, $\phi_c = \sqrt{\lambda/\lambda'}M$, after which χ becomes unstable (the effective mass-squared becomes negative) and rapidly rolls down towards one of the true minima at $\chi = \pm\chi_0$. Then ϕ goes to zero and starts to oscillate while χ will reach the true minimum. Inflation will end either with the instability or because of the end of slow-roll, as in the single field case, depending on which occurs first.

Before ϕ reaches ϕ_c we can write the potential as a function of ϕ only,

$$V(\phi) = M^4 + \frac{1}{2}m^2\phi^2, \quad (2)$$

where we wrote the false vacuum energy density $\frac{1}{4}\lambda\chi_0^4$ as just M^4 . We define the ratio between the false vacuum energy density and the inflaton energy density as

$$E(\phi) = \frac{M^4}{\frac{1}{2}m^2\phi^2}. \quad (3)$$

So if $E \gtrsim 1$ we have false vacuum dominated inflation and if $E \ll 1$ we have almost chaotic inflation [8].

A. The dynamics

The dynamics of hybrid inflation are given by the equation of motion of the inflaton (we are assuming that the “waterfall” field stays at the origin, so it does not evolve) and the Friedmann equation,

$$\ddot{\phi} + 3H\dot{\phi} = -V'(\phi), \quad (4)$$

*email: Antonio.Cardoso@port.ac.uk

$$H^2 = \frac{8\pi}{3m_{Pl}^2} \left(\frac{1}{2}\dot{\phi}^2 + V(\phi) \right), \quad (5)$$

where $H = \dot{a}/a$ is the Hubble parameter, a is the scale factor, m_{Pl} is the Planck mass (which we set equal to 1), a dot represents a derivative with respect to time and a prime denotes a derivative with respect to the field ϕ . We will use the slow-roll approximation for our calculations, which is given by the conditions

$$\epsilon(\phi) \equiv \frac{m_{Pl}^2}{16\pi} \left(\frac{V'(\phi)}{V(\phi)} \right)^2 \ll 1, \quad (6)$$

$$\eta(\phi) \equiv \frac{m_{Pl}^2}{8\pi} \frac{V''(\phi)}{V(\phi)} \ll 1. \quad (7)$$

With these approximations, Eqs. (4) and (5) can be written as

$$3H\dot{\phi} \simeq -V'(\phi), \quad (8)$$

$$H^2 \simeq \frac{8\pi}{3m_{Pl}^2} V(\phi, \chi). \quad (9)$$

Then we can write, for the number of e-folds of expansion between two field values ϕ_1 and ϕ_2 ,

$$N(\phi_1, \phi_2) \equiv \ln \frac{a_2}{a_1} \simeq -\frac{8\pi}{m_{Pl}^2} \int_{\phi_1}^{\phi_2} \frac{V(\phi)}{V'(\phi)} d\phi. \quad (10)$$

For the potential in Eq. (2) we have

$$\eta(\phi) = \frac{m^2 m_{Pl}^2}{4\pi(2M^4 + m^2\phi^2)}, \quad (11)$$

$$\epsilon(\phi) = \frac{m^4 \phi^2 m_{Pl}^2}{4\pi(2M^4 + m^2\phi^2)^2} = \frac{1}{2} \frac{8\pi}{m_{Pl}^2} \eta^2 \phi^2, \quad (12)$$

$$N(\phi_1, \phi_2) \simeq \frac{8\pi M^4}{m^2 m_{Pl}^2} \ln \frac{\phi_1}{\phi_2} + \frac{2\pi}{m_{Pl}^2} (\phi_1^2 - \phi_2^2). \quad (13)$$

When the end of slow-roll occurs before the inflaton reaches ϕ_c we identify the end of inflation with the condition $\epsilon = 1$, which occurs for the value of the inflaton field [3]

$$\phi_\epsilon = \frac{m_{Pl}}{\sqrt{16\pi}} \left(1 + \sqrt{1 - \frac{32\pi}{m_{Pl}^2} \frac{M^4}{m^2}} \right). \quad (14)$$

There is a second root at a smaller ϕ , below which ϵ becomes smaller than unity again, but numerically it has been found that slow-roll is not re-established before $\phi = 0$ [3].

We see that if $32\pi M^4 / m_{Pl}^2 m^2 > 1$ then ϕ_ϵ does not exist at all, so in this case inflation has to end by instability. If $32\pi M^4 / m_{Pl}^2 m^2 \leq 1$ it will end by instability when $\phi = \phi_c$ if $\phi_c > \phi_\epsilon$ or by the end of slow-roll when $\phi = \phi_\epsilon$ if $\phi_\epsilon > \phi_c$.

We assume that cosmological scales exit the Hubble scale at least 50 e-folds before the end of inflation. In practice the actual number of e-folds is dependent upon

the details of reheating at the end of inflation. Given that ϕ_c can be made arbitrarily small by suitable choice of λ/λ' we leave ϕ_{50} , the value of ϕ when cosmological scales leave the Hubble scale, as a free parameter to be determined by observations, subject only to the restriction that we must have at least 50 e-folds between ϕ_{50} and ϕ_ϵ . If ϕ_ϵ does not exist then we can always have at least 50 e-folds and any value of ϕ_{50} is allowed.

B. The perturbations

The power spectrum of scalar curvature perturbations at horizon crossing (when the comoving scale k equals the Hubble radius, $k = aH$, during inflation), which is conserved on large scales in single field inflation, is given by, to leading order in the slow-roll parameters, [9]

$$\mathcal{P}_R(k) = \left(\frac{H^2}{2\pi\dot{\phi}} \right)^2 \Big|_*, \quad (15)$$

where the subscript $*$ indicates that the quantity is to be evaluated at horizon crossing. By virtue of the slow-roll conditions this formula gives a value of \mathcal{P}_R which is nearly independent of k . For the potential in Eq. (2), assuming slow-roll, Eq. (15) can be written as, using Eqs. (6), (8), (9), (2) and (12),

$$\mathcal{P}_R = \frac{16\pi}{3} \frac{(2M^4 + m^2\phi_{50}^2)^3}{m_{Pl}^6 m^4 \phi_{50}^2}. \quad (16)$$

So for each values of M and m we can find the values of ϕ_{50} (there are several possible values for each combination of M and m) which satisfy the density perturbation amplitude, for scales of cosmological interest, from the WMAP three-year results [1] (assuming that the running of the spectral tilt is zero).

The spectral tilt for the scalar curvature perturbations, the running of the spectral tilt and the tensor to scalar ratio can be written as, to leading order in the slow-roll parameters, [9]

$$n_s = 1 - 6\epsilon_* + 2\eta_*, \quad (17)$$

$$\alpha_s = 16\epsilon_* \eta_* - 24\epsilon_*^2 + 2\xi_*^2, \quad (18)$$

$$r = 16\epsilon_*, \quad (19)$$

where ξ is a higher order slow-roll parameter and is equal to zero for our specific potential, Eq. (2). Then for this potential we can write

$$n_s = 1 + \frac{m_{Pl}^2 m^2 (M^4 - m^2 \phi_{50}^2)}{\pi (2M^4 + m^2 \phi_{50}^2)^2}, \quad (20)$$

$$\alpha_s = \frac{m_{Pl}^4 m^6 \phi_{50}^2 (4M^4 - m^2 \phi_{50}^2)}{2\pi^2 (2M^4 + m^2 \phi_{50}^2)^4}, \quad (21)$$

$$r = \frac{4m_{Pl}^2 m^4 \phi_{50}^2}{\pi (2M^4 + m^2 \phi_{50}^2)^2}. \quad (22)$$

C. Results and discussion

We have run a code to calculate numerically ϕ_{50} , E and the parameters n_s , r and α_s at Hubble crossing (when $\phi = \phi_{50}$), assuming slow-roll and using the definitions and results from the previous sections, for m between 10^{-4} and 10^{-8} and M between 10^{-2} and 10^{-5} . For each values of m and M we have selected the value of ϕ_{50} such that the amplitude of the scalar curvature perturbations Eq. (16) obeys the WMAP three-year results [1]. We discard the cases for which the number of e-folds between ϕ_{50} and ϕ_ϵ is smaller than 50 and those with a blue spectrum, i.e., we require $n_s < 1$. The energy density ratio, Eq. (3), is evaluated at ϕ_{50} .

We first note that as one goes from larger to smaller values of M the density of points selected by the code gets larger because the selection of the values of M is logarithmic, as one can see looking to the plot in Figure 1.

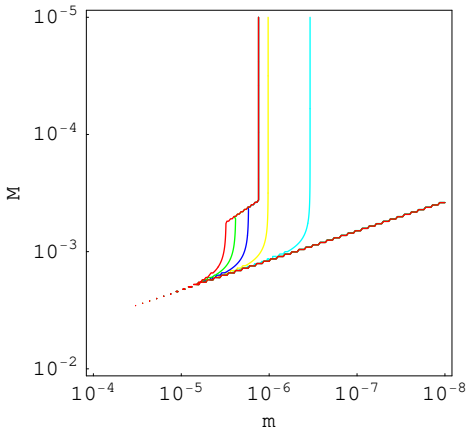


FIG. 1: Contour plot of n_s as a function of m and M for $0.9 < n_s < 1$, for the hybrid inflation model. The red, green, blue, yellow and light blue contours (from left to right) represent, respectively, n_s equal to 0.91, 0.93, 0.95, 0.97 and 0.99.

Analyzing the top plot in Fig. 2 we see that there is a small range of parameters for which (n_s, r) is inside the 68% confidence level contour from WMAP only [5]. For this range we find

$$0.9525 \lesssim n_s \lesssim 0.9975 \quad \text{and} \quad 0.05 \lesssim r \lesssim 0.35. \quad (23)$$

For the range of parameters for which (n_s, r) is inside the 95% confidence level contour we find

$$0.94 \lesssim n_s \lesssim 1 \quad \text{and} \quad 0 \lesssim r \lesssim 0.55. \quad (24)$$

Considering the results from WMAP + SDSS [5] we see that, looking to the bottom plot in Fig. 2, the range of parameters for which (n_s, r) is inside the 68% confidence level contour is smaller than in the previous case. For this range we find

$$0.96 \lesssim n_s \lesssim 0.995 \quad \text{and} \quad 0.05 \lesssim r \lesssim 0.175. \quad (25)$$

For the range of parameters for which (n_s, r) is inside the 95% confidence level contour we have

$$0.95 \lesssim n_s \lesssim 1 \quad \text{and} \quad 0 \lesssim r \lesssim 0.3. \quad (26)$$

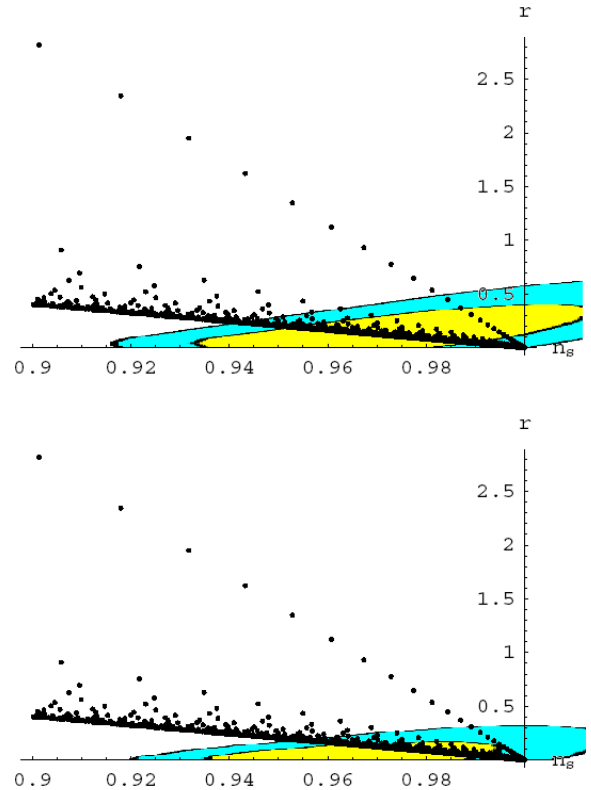


FIG. 2: Plots of r as a function of n_s for $0.9 < n_s < 1$ (the black dots represent the different values of M and m), for the hybrid inflation model, with the 68% (yellow) and 95% (blue) confidence level contours from WMAP (top) and WMAP + SDSS (bottom), taken from [5].

Observing the plot in Figure 3 we see that the closer one gets to large values of M the larger are the values of r (i.e., the energy scale of inflation increases when M increases) and α_s . Analyzing the plot in Figure 4 we see that the closer one gets to small values of ϕ_{50} the larger are the values of r (and so also the values of α_s get larger). We also note that ϕ_{50} is never much smaller than 1, i.e., the Planck mass. Looking to the plot in Figure 5 we note that the energy density ratio is never much larger than 1, which means that there is never a real false vacuum domination of the energy density, otherwise we would have $n_s \geq 1$. We also see that the closer one gets to the false vacuum domination cases (which occur for large values of M) the larger are the values of r and the larger (and positive) are the values of the the running α_{50} .

From this analysis we see that when we have false vacuum domination and small values of ϕ_{50} , i.e., when we

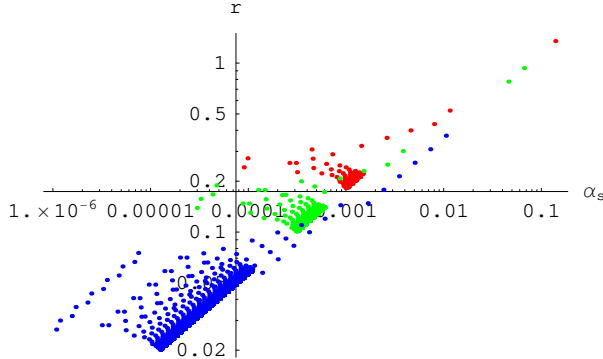


FIG. 3: Plot of r as a function of α_s for $0.945 < n_s < 0.955$ (red), $0.965 < n_s < 0.975$ (green) and $0.985 < n_s < 0.995$ (blue), for the hybrid inflation model.

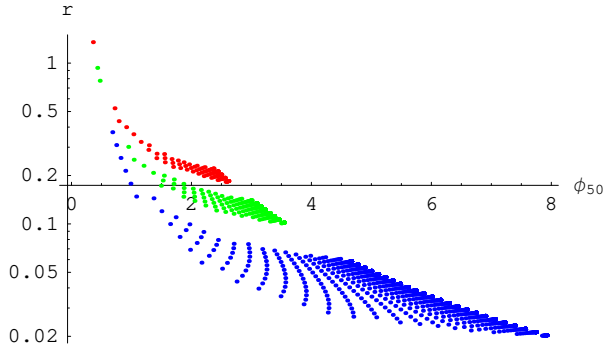


FIG. 4: Plot of r as a function of ϕ_{50} for $0.945 < n_s < 0.955$ (red), $0.965 < n_s < 0.975$ (green) and $0.985 < n_s < 0.995$ (blue), for the hybrid inflation model.

are more distant from chaotic inflation, then the values of the the running α_{50} are large and positive, which is in contradiction with the WMAP three-year results [5]. Also the values of the tensor to scalar ratio r tend to be very large for these cases, which is also in disagreement with the observations.

When M goes to very small values we recover the results for chaotic inflation, which correspond to the lower limit for r along the values of n_s in Fig. 2. For these cases, for which ϕ_{50} is very large and the energy density ratio very small, we have small values for α_{50} and r , which is in very good agreement with the WMAP three-year results [5].

III. CONCLUSIONS

We have found that there is an intermediate regime for the original hybrid inflation model compatible with $n_s < 1$, but as one approaches the false vacuum dominated limit within this regime the tensor-to-scalar ratio, r , and

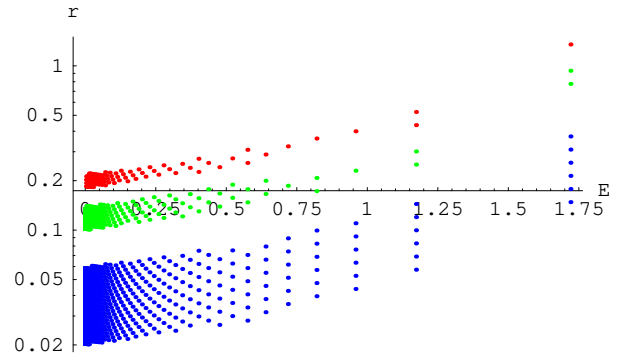


FIG. 5: Plot of r as a function of E for $0.945 < n_s < 0.955$ (red), $0.965 < n_s < 0.975$ (green) and $0.985 < n_s < 0.995$ (blue), for the hybrid inflation model.

the running of the spectral tilt, α_s , become large (with a positive running), which is in contradiction with the WMAP three-year results [5]. We found a lower bound on the allowed values of r , which might be an observational signal for hybrid inflation because if there is an upper bound on the spectral index, $n_s < 1$, then we find a lower bound on the tensor to scalar ratio, r . This lower bound corresponds to chaotic inflation, which is in very good agreement with the WMAP three-year results [5]. At the same time we saw that it is difficult to get ϕ_{50} smaller than the Planck scale in this model because decreasing ϕ_{50} requires us to increase the vacuum energy scale, M , and this increases the tensor-to-scalar ratio, r .

The inverted hybrid inflation model (see Appendix) is in much better agreement with the WMAP three-year results [5] than the original hybrid inflation model when we consider the false vacuum dominated regimes, especially because there is no lower bound on the allowed values of r . Moreover, in the inverted hybrid model there is no problem obtaining small values for $\phi_{50} \ll 1$, which makes these model easier to implement within supergravity [4].

Acknowledgements

I would like to thank David Wands for very useful discussions and comments on this work. I would also like to thank the authors of Ref. [5] for permission to reproduce likelihood contours from their work. I am supported by FCT (Portugal) PhD fellowship SFRH/BD/19853/2004.

APPENDIX: THE INVERTED HYBRID INFLATION MODEL

If we invert the sign of the inflaton energy density in Eq. (2) we get

$$V(\phi) = M^4 - \frac{1}{2}m^2\phi^2, \quad (27)$$

which corresponds to the potential for the inverted hybrid inflation model with a quadratic potential for the inflaton. A particular case of this model are the small-field inflation models [9], for which the potential in Eq. (27) corresponds to a Taylor expansion about the origin and higher order terms are required to provide a potential minimum at some $\phi \neq 0$, as required to connect to a reheating stage (which is necessary to make the model realistic). So the inflaton starts with an initial small (positive) value and rolls down towards the minimum at a larger value, then it starts to oscillate and inflation ends with the end of slow-roll.

All the equations obtained before for the original hybrid inflation model, except Eq. (14), are still valid but with m^2 replaced by $-m^2$. To find the value of ϕ_ϵ we search for the solutions of Eq. (12) with ϵ equal to 1 (there are two different solutions for this equation but the results do not depend on which solution we choose).

1. Results and discussion

In this case we have run the same code (with the appropriate changes in the equations) but for m between 10^{-4} and 10^{-10} and M between 10^{-2} and 10^{-6} . The energy density ratio, Eq. (3), is evaluated 50 e-folds after the inflaton has the value ϕ_{50} .

Note that also in this case the selection of the values of M is logarithmic, as one can see looking to the plot in Figure 6.

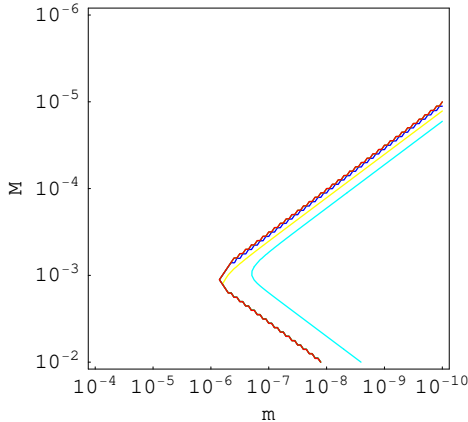


FIG. 6: Contour plot of n_s as a function of m and M for $0.9 < n_s < 1$, for the inverted hybrid inflation model. The red, green, blue, yellow and light blue contours (from left to right) represent, respectively, n_s equal to 0.91, 0.93, 0.95, 0.97 and 0.99.

Analyzing the top plot in Fig. 7 we see that there is a much wider range of parameters for which (n_s, r) is inside the 68% confidence level contour from WMAP only [5] than in the original hybrid case, especially because there

is no lower bound on the allowed values of r , in contrast with the original hybrid inflation model. For this range we find

$$0.935 \lesssim n_s \lesssim 0.9875 \quad \text{and} \quad 0 \lesssim r \lesssim 0.0775. \quad (28)$$

For the range of parameters for which (n_s, r) is inside the 95% confidence level contour we get

$$0.9175 \lesssim n_s \lesssim 1 \quad \text{and} \quad 0 \lesssim r \lesssim 0.0775. \quad (29)$$

Observing the bottom plot in Fig. 7 we can see that there is also a wide range of parameters for which (n_s, r) is inside the 68% confidence level contour from WMAP + SDSS [5]. For this range we get

$$0.935 \lesssim n_s \lesssim 0.9925 \quad \text{and} \quad 0 \lesssim r \lesssim 0.0775, \quad (30)$$

and for the range of parameters for which (n_s, r) is inside the 95% confidence level contour we find

$$0.92 \lesssim n_s \lesssim 1 \quad \text{and} \quad 0 \lesssim r \lesssim 0.0775. \quad (31)$$

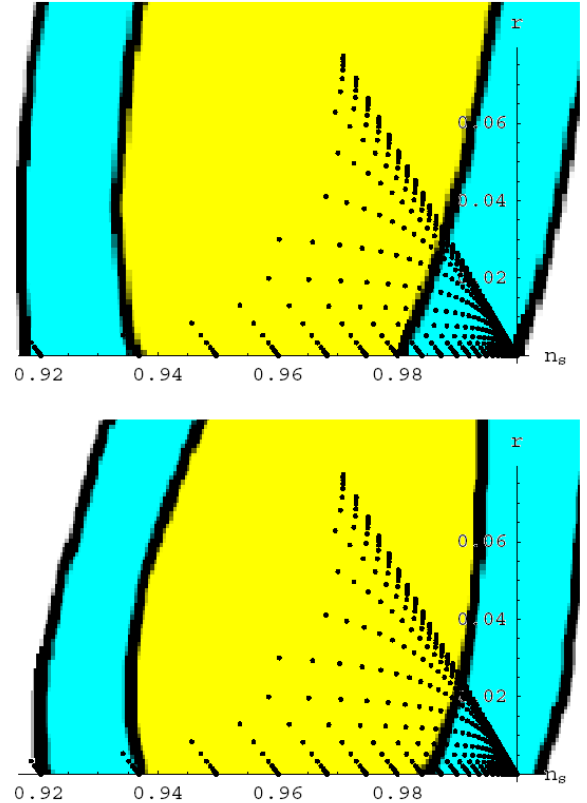


FIG. 7: Plots of r as a function of n_s for $0.9 < n_s < 1$ (the black dots represent the different values of M and m), for the inverted hybrid inflation model, with the 68% (yellow) and 95% (blue) confidence level contours from WMAP (top) and WMAP + SDSS (bottom), taken from [5].

Looking to the plot in Figure 8 we see that the closer one gets to large values of M the smaller are the values of r and α_s (although we note that they are always small, even in the cases for which M is small). Analyzing the plot in Figure 9 we see that the closer one gets to small values of ϕ_{50} the smaller are the values of r (and so also the values of α_s get smaller). We note that here ϕ_{50} can be much smaller than the Planck mass. Observing the plot in Figure 10 we see that the closer one gets to the more false vacuum domination cases (which occur for large values of M) the smaller are the values of r (and so also the values of α_s). In this case we note that the energy density ratio can be very large, so we can have a strong vacuum domination.

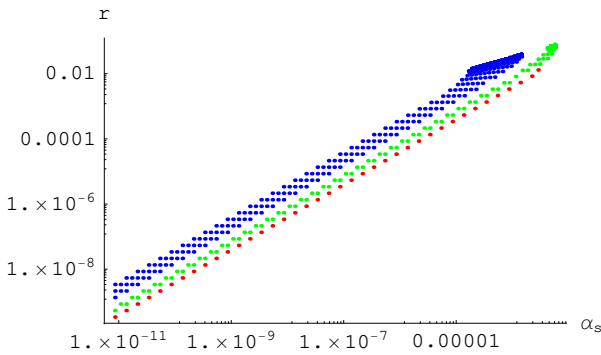


FIG. 8: Plot of r as a function of α_s for $0.945 < n_s < 0.955$ (red), $0.965 < n_s < 0.975$ (green) and $0.985 < n_s < 0.995$ (blue), for the inverted hybrid inflation model.

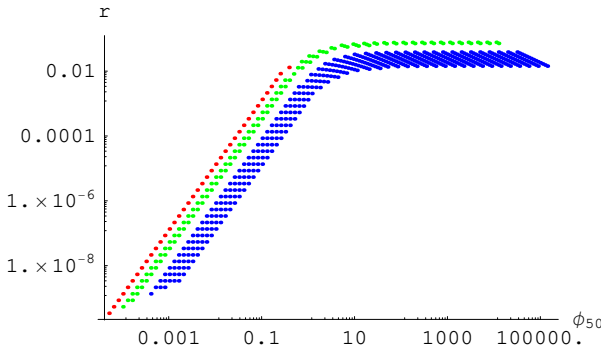


FIG. 9: Plot of r as a function of ϕ_{50} for $0.945 < n_s < 0.955$ (red), $0.965 < n_s < 0.975$ (green) and $0.985 < n_s < 0.995$ (blue), for the inverted hybrid inflation model.

From the previous analysis we see that for the inverted hybrid inflation model we can have, specially for large M , very small values for r and α_s , which is in very good agreement with the WMAP three-year results [5]. For these cases ϕ_{50} is also very small (it can be much smaller than 1, i.e., the Planck mass) and E is much larger than 1, which means that there is a large false vacuum domination of the energy density. Therefore we can conclude that this model is in much better agreement with the WMAP results than the original hybrid inflation model when we consider the false vacuum domination regimes, especially because there is no lower bound on the allowed values of r . Moreover, in this model there is no problem obtaining small values for $\phi_{50} \ll 1$, which makes these model easier to implement within supergravity [4].

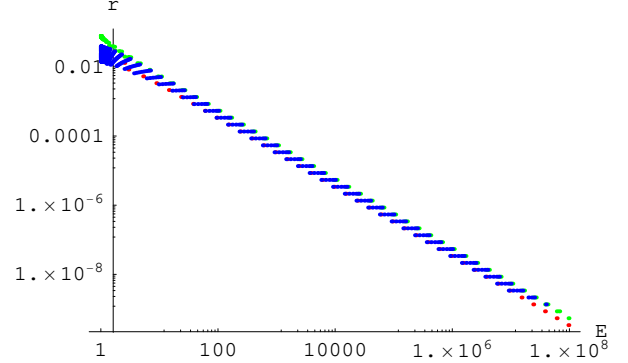


FIG. 10: Plot of r as a function of E for $0.945 < n_s < 0.955$ (red), $0.965 < n_s < 0.975$ (green) and $0.985 < n_s < 0.995$ (blue), for the inverted hybrid inflation model.

[1] D. N. Spergel *et al.*, arXiv:astro-ph/0603449.
[2] A. D. Linde, Phys. Rev. D **49** (1994) 748 [arXiv:astro-ph/9307002].
[3] E. J. Copeland, A. R. Liddle, D. H. Lyth, E. D. Stewart and D. Wands, Phys. Rev. D **49** (1994) 6410 [arXiv:astro-ph/9401011].
[4] D. H. Lyth and A. Riotto, Phys. Rept. **314** (1999) 1 [arXiv:hep-ph/9807278].
[5] W. H. Kinney, E. W. Kolb, A. Melchiorri and A. Riotto,

Phys. Rev. D **74** (2006) 023502 [arXiv:astro-ph/0605338].
[6] H. J. de Vega and N. G. Sanchez, arXiv:astro-ph/0604136.
[7] D. H. Lyth and E. D. Stewart, Phys. Rev. D **54** (1996) 7186 [arXiv:hep-ph/9606412].
[8] A. D. Linde, Phys. Lett. B **129** (1983) 177.
[9] B. A. Bassett, S. Tsujikawa and D. Wands, arXiv:astro-ph/0507632.